Rugged lava flows on the Moon revealed by Earth-based radar

Bruce A. Campbell,[1] B. Ray Hawke,[2] Lynn M. Carter,[1] Rebecca R. Ghent,[3] and Donald B. Campbell[4]

[1] Basaltic volcanism is widespread on the lunar nearside, and returned samples suggest that the mare-forming magmas had low viscosity that led to primarily sheet-like deposits. New 70-cm wavelength radar observations that probe several meters beneath the lunar surface reveal differences in mare backscatter properties not explained by age or compositional variations. We interpret areas of high backscatter and high circular polarization ratio in Maria Serenitatis, Imbrium, and Crisium as having an enhanced abundance of decimeter-scale subsurface rocks relative to typical mare-forming flows. The 3.5 b.y survival of these differences implies an initial platy, blocky, or ridged lava flow surface layer with thickness of at least $3-5$ m. Such rugged morphology might arise from episodic changes in magma effusion rate, as observed for disrupted flood basalt surfaces on the Earth and Mars, very high flow velocities, or increased viscosity due to a number of factors. Significant information on lunar mare eruption conditions may thus be obtained from long-wavelength radar probing of the shallow subsurface. **Citation:** Campbell, B. A., B. R. Hawke, L. M. Carter, R. R. Ghent, and D. B. Campbell (2009), Rugged lava flows on the Moon revealed by Earth-based radar, *Geophys. Res. Lett.*, *36*, L22201, doi:10.1029/2009GL041087.

1. Introduction

[2] Impact basins on the nearside of the Moon are filled by basaltic lava, and analysis of returned samples shows that many flows had very low viscosity relative to terrestrial basalts [*Weill et al.*, 1971; *Rutherford et al.*, 1974]. While some large lobate fronts are visible, most flows are 10 m or less in thickness [*Schaber et al.*, 1976; *Gifford and El-Baz*, 1981], and smooth at the 10's of meter horizontal scale. Impact bombardment has produced a regolith that thickens with increasing age, from about 4 m to 10 m, atop all mare units [*McKay et al.*, 1991]. The inferred low viscosity, thin flow units, and minimal relief all suggest that mare flows were also relatively smooth at the meter scale upon emplacement, but this conclusion is influenced by the presence of the regolith, which subdues local topography and masks any residual morphologic differences in the basal terrain.

[3] Since the regolith is less dense than rock by up to a factor of two [*Carrier et al.*, 1991], at least $2-5$ m of material from the top of a bedrock unit must be pulverized and mixed. Differences in flow surface roughness comparable, for example, to the distinctions between pahoehoe and aa in terrestrial basalts should be erased in this process, leaving a regolith rock population relatively independent of the initial flow morphology for any given emplacement age. Recent work on the radar scattering properties of domes in the Marius Hills region, however, suggests that very rugged flow structures persist beneath the regolith cover [*Campbell et al.*, 2009], so it is reasonable to search for similarly surviving variations within the mare units. In this work, we combine new 70-cm radar data with titanium abundances inferred from Clementine multi-spectral data to minimize compositional effects on the backscattered signal, and investigate the remaining differences among mare units for their possible relationship to age and flow morphology.

2. Radar, Multi-spectral, and Crater Age Data

[4] The new 70-cm radar data were collected using the Arecibo Observatory transmitter and receivers at the Green Bank Telescope. Coverage of most nearside maria was acquired with a best spatial resolution of 450 m per pixel [*Campbell et al.*, 2007]. A higher-resolution (about 200 m per pixel) image for the northeastern nearside was obtained by using a shorter (1 μs) pulse and proportionally longer integration time. The transmitted signal is circularly polarized, and the reflected echoes were received in both the same circular sense as that transmitted (SC) and in the opposite sense (OC). The ratio of the SC to the OC components is termed the circular polarization ratio (CPR), or μ_c.

[5] Reflectance spectra and returned samples reveal significant variability in the FeO and TiO_2 content of mare-forming basalts, with titanium differences causing strong visible-UV contrasts [*Whitaker*, 1972; *Lucey et al.*, 2000; *Gillis et al.*, 2003]. Comparison of color-difference images with early 70-cm data showed an inverse correlation between the blue tone of deposits in Mare Imbrium and their SC radar returns, attributed to attenuation of diffuse echoes from subsurface rocks (i.e., a smaller radar penetration depth) by the high-microwave-loss mineral ilmenite ($FeTiO_3$) [*Schaber et al.*, 1975; *Carrier et al.*, 1991]. The decrease in SC echo strength with increasing titanium content was later found to apply to other mare deposits [*Campbell et al.*, 1997].

[6] Here we use the CPR to characterize diffuse scattering, since it is strongly modulated by changes in the abundance of rocks, on or beneath the lunar surface, with diameters of about 1/10 the radar wavelength and larger, and is more readily calibrated than the absolute backscatter cross section [*Campbell et al.*, 2007]. We examined data for Maria Humorum, Crisium, Serenitatis, and Imbrium to derive an empirical relationship between the radar incidence

[1]Center for Earth and Planetary Studies, Smithsonian Institution, Washington, D. C., USA.
[2]HIGP, University of Hawai'i at Mānoa, Honolulu, Hawaii, USA.
[3]Department of Geology, University of Toronto, Toronto, Ontario, Canada.
[4]NAIC, Cornell University, Ithaca, New York, USA.
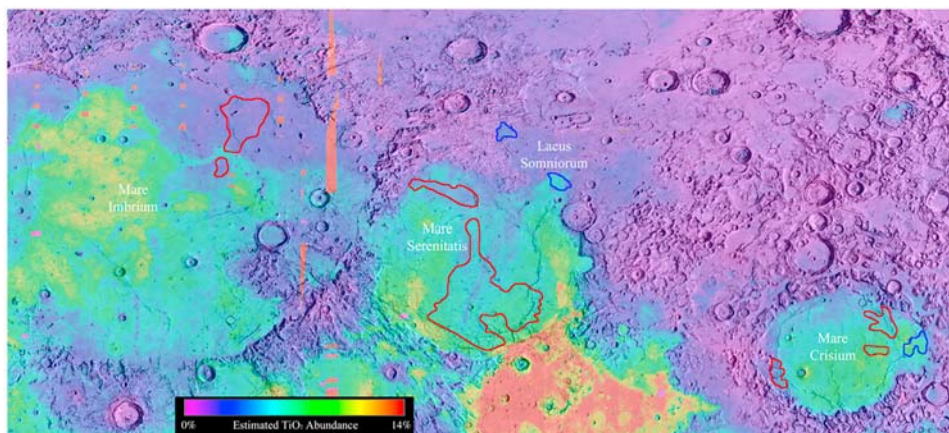
Figure 1. Shaded-relief map of three lunar mare basins, with color overlay of estimated TiO_2 abundance. Approximate outlines of areas sampled for the plot in Figure 2 as representative of high adjusted circular polarization ratio (CPR) values shown in red, and those with low adjusted CPR values shown in blue. Floor of crater Billy (13.8°S, 50.1°W) also included in low-CPR samples, but not shown here. Region covered 7°N to 55°N, 34°W to 72°E.

angle, φ, model-derived TiO_2 content [*Gillis et al.*, 2003], and 70-cm CPR. The dependence of the angle-normalized CPR on TiO_2 abundance (in percent) is well represented, for $\varphi = 30°-80°$, by:

$$\frac{\mu_c}{(0.04 + 0.0068\phi)} = 1.1\exp[-0.081*TiO_2]. \quad (1)$$

[7] This relationship was then used to minimize the effect of TiO_2 content on the CPR in order to explore the possible role of mare age or other factors on diffuse radar echoes. Relative ages of mare units are constrained by the population of impact craters in the $0.5-2$ km diameter range, and absolute calibration is provided by returned samples [e.g., *Hiesinger et al.*, 2000, 2003].

3. Results and Interpretation

[8] While there is a continuum of TiO_2-adjusted CPR values across the four studied maria, two distinct groups of sites (Figure 1) with very low and very high adjusted-CPR values are readily identified, and we averaged over areas of a few hundred km^2 within these sites to obtain the sample points presented in Figure 2. The two populations generally follow the best-fit trend for the nearside maria, but with a multiplicative offset of about ±2.5 dB. With the exception of a patch in east-central Crisium, high-CPR deposits are only evident at relatively low TiO_2 content (<6%), whereas the lower-CPR group comprises terrain with abundances up to at least 10%.

[9] Mare age differences are a possible source of strong variability in diffuse radar backscatter, based on analogy to eclipse thermal maps that show surface rock abundance variations [*Shorthill*, 1973]. In this model, older deposits have a thicker, rock-poor regolith and low radar echoes relative to young, radar-bright terrain. While this mechanism likely occurs at some level, it does not explain the dramatic offsets from the average 70-cm CPR-TiO_2 behavior noted in Figure 2. Some of the highest-CPR units in Mare Serenitatis are dated at approximately 3.5 b.y. [*Hiesinger et al.*, 2000], and crater counts by the current authors, *Hackwill et al.*

[2006], and *Heisinger et al.* [2003] for several of the low-CPR (and thus putatively older) units show a range of ages from about 1.7 to 3.1 b.y. It is also possible a mineral other than ilmenite has a strong effect on the microwave loss tangent, leading to offsets from the average trend. It seems unlikely, however, that a sampling of sites with high-CPR and low-CPR characteristics would exhibit such general agreement with the slope of the TiO_2 dependence (Figure 2) – in effect, the unknown mineral would have to occur in direct proportion to ilmenite in all locations.

[10] Based on the lack of correlation between the radar properties and mare age or ilmenite content, we propose that
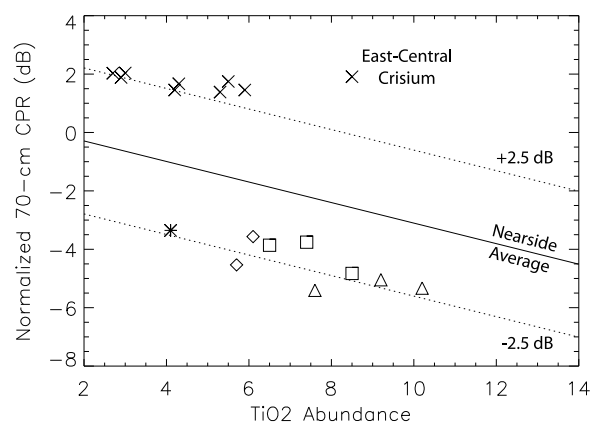
Figure 2. The 70-cm circular polarization ratio normalized for incidence angle, in decibels, versus TiO_2 abundance estimated from Clementine multi-spectral data. Solid line shows average behavior of nearside maria; dotted lines are offset by ±2.5 dB from this trend, approximately coincident with behaviors of low- and high-CPR mare deposits. High-CPR points (crosses) drawn from sample regions in Maria Imbrium, Serenitatis, and Crisium (Figure 1). Low-CPR plot symbols correspond to patches in Lacus Somniorum (asterisk), the Billy crater floor (triangles), eastern Mare Crisium (squares), and NE Mare Serenitatis north of Posidonius crater (diamonds).
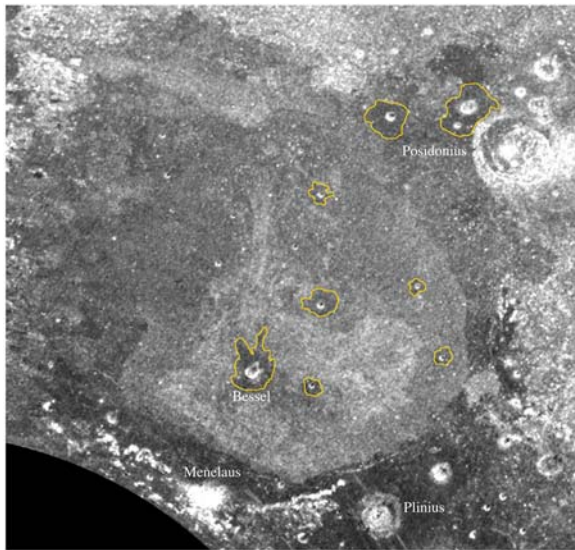
Figure 3. The 70-cm wavelength circular polarization ratio (CPR) for Mare Serenitatis (14°N–38°N, 7°E–33°E; image width about 790 km). Data averaged to 2.2-km resolution to reduce speckle noise to <10% of CPR values. Range of tones corresponds to CPR of ∼0.1 to greater than unity (shown as white). No correction made for TiO_2 content of materials. Yellow outlines show low returns associated with fine ejecta deposits of younger craters. Note the extensive region of higher CPR values north and east of Bessel, which we attribute to enhanced regolith rock abundance.

the residual differences in TiO_2-adjusted CPR values reflect variations in the population of decimeter-scale and larger diameter rocks, on the mare surface or buried within the probing depth of the radar signal, due to some other geologic mechanism. The radar returns could arise in part from the transition zone between the regolith and the remaining intact bedrock if the total integrated attenuation is relatively low. Whether this transition zone has a different rock population than the well-mixed overlying material is unknown, and could depend upon the physical properties of the original lava flows.

[11] Evidence for detection of subsurface physical characteristics comes from analysis of the 1-μs 70-cm data for Mare Serenitatis, where the CPR map (Figure 3) shows a high degree of variability that is not well correlated with estimated TiO_2 abundance (Figure 4); these properties are also evident in earlier 70-cm radar and color difference analyses [*Thompson et al.*, 1974]. In particular, there is a central high-CPR region that extends 275 km north and 230 km east of Bessel crater, terminating in numerous finger-like or lobate features. These radar-bright features do not everywhere follow the boundaries of units defined on the basis of multi-spectral properties (i.e., TiO_2 or FeO content), suggesting that they may reflect morphologic variations within a more extensive flow complex. Another high-CPR region extends approximately ESE-WNW across the north-western quadrant of the basin. The regolith rock abundance in these areas is substantially enhanced relative to mare deposits of similar TiO_2 content; the area of highest CPR in southern Mare Serenitatis has an average SC backscatter

coefficient 5 dB (a factor of 3) greater than nearby mare units and only 5 dB below that of rugged ejecta from the young crater Copernicus.

[12] The high-CPR feature in southern and central Serenitatis (Figure 3) occurs within a region of generally uniform, low TiO_2 abundance, with the exception of lower-titanium streaks we infer to be highland material excavated by nearby and perhaps distant craters (Figure 4). This broad region was dated based on crater degradation characteristics to 3.4–3.6 b.y. [*Boyce*, 1976]. Galileo multi-spectral data were used to map three mare units across the high-CPR area, with estimated ages of 3.49, 3.44, and, anomalously, 2.84 b.y. [*Hiesinger et al.*, 2000]. Given the subtle nature of the multi-spectral differences used to define these three mare units, and the evident role of contamination by high-lands material, we suggest that the radar identifies a single flow complex whose average age is 3.4–3.6 b.y. The high-CPR feature in NW Serenitatis is correlated with a mapped unit of estimated age 3.37 b.y [*Hiesinger et al.*, 2000].

[13] The differences between the 70-cm radar returns and estimated TiO_2 abundance in southern Mare Serenitatis are not mirrored in 12.6-cm wavelength CPR values [*Carter et al.*, 2009], which are relatively low in the region immediately surrounding Bessel crater. The 12.6-cm returns and CPR are lowest where the TiO_2 content is very high, but in moderate-TiO_2 units age may play an equally important role in modulating the cm-scale rocks that dominate the diffuse backscattered return. For any given loss tangent the expected radar penetration distance increases by about a factor of five from 12.6-cm to 70-cm wavelength, so the inferred enhancements in regolith rock abundance likely occur below the probing depth of the higher-frequency signal. Such a deeper source region for the strong 70-cm diffuse echoes is also consistent with the observation of
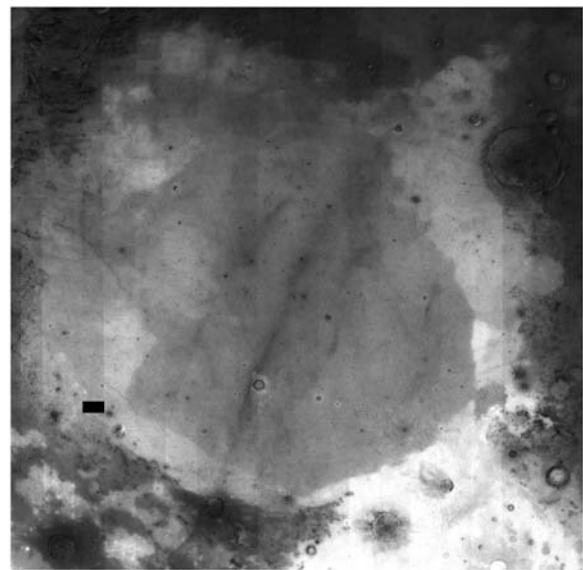
Figure 4. Regolith abundance of TiO_2 based on Clementine multi-spectral data, shown as a greyscale image (0–15% abundance) for the region in Figure 3. Note the lack of any strong correlation between radar-observed features north and east of Bessel crater and the chemistry of the mare-forming flows.

high-CPR features where the estimated TiO_2 content is less than about 6%, corresponding to maximum regolith loss tangent values of 0.01 [*Carrier et al.*, 1991]. The detection of a high-CPR signature at ~9% TiO_2 content in eastern Crisium correlates with terrain mapped by *Casella and Binder* [1972] as "rough mare material", characterized by ridge- and dome-like features and inferred to form by localized eruptions. We propose that high CPR values in this area correspond to an even more rugged (e.g., blocky) lava flow morphology, similar to that of the Marius domes [*Campbell et al.*, 2009].

4. Discussion

[14] The lunar radar data show that rugged interfaces or greatly enhanced subsurface rock populations, within the probing depth of the 70-cm signal, occur across significant mare regions, but cannot further constrain the original flow morphology (blocky, slabby, ridged, etc.) that gave rise to these differences after billions of years of impact bombardment. The process of regolith development will erase morphologic diversity at the 1–2 m vertical scale between mare lava flow units. On Earth, this scale range characterizes the difference between sheet-like or platy pahoehoe and jagged aa terrain in Hawaiian basalts. Our observations imply substantially greater relief for the blocky, slabby, or otherwise rugged layer atop the initial lunar flows, such that the comminution of material 2–5 m down simply exposes additional rough terrain.

[15] Such large-scale relief does not require magmas more silicic than basalt, as shown by occasional examples of blocky deposits such as SP flow in Arizona [*Schaber et al.*, 1980] and, perhaps more important as a mare analogy, by the occurrence of very rough, "rubbly" pahoehoe terrain in Icelandic flood basalts [*Keszthelyi et al.*, 2004]. Based on field observations, *Keszthelyi et al.* [2004] suggest that a flow crust formed above a moving layer of magma is broken apart and entrained by surges in the eruption rate, forming a rugged jumble of fragments several meters thick. They further identify flow complexes on Mars with similar morphology to that of the Icelandic platy and ridged units. The same texture might occur in a more rapidly emplaced flow unit where the cooled crust is repeatedly broken up to form a thick layer above the mobile core. Radar echoes from blocky flows on Earth and the inferred platy/ridged flows on Mars are higher than those of aa surfaces, with CPR values approaching unity [*Campbell et al.*, 2009; *Harmon et al.*, 1999], so they appear to be good analogs for the central Serenitatis and other "rough" deposits. The formation of rough mare flows may occur by such variations in eruption conditions, though increased magma viscosity due to alkalinity [*Weill et al.*, 1971], temperature, or other factors is another plausible mechanism.

[16] In contrast, areas of very low CPR are inferred to be rock-poor relative to the average mare regolith of similar age and ilmenite content. The reason for a paucity of suspended rocks is uncertain; possibilities include the presence of earlier pyroclastic debris beneath thin flow units that are now mixed to form a regolith of lower rock abundance. It is also possible that the algorithm used to infer TiO_2 abundance is biased downward in these deposits by some other mineral that has no effect on the radar echoes.

[17] These observations offer a new window on the evolution of lunar magma sources over time. High-resolution photography, particularly at low Sun angles, may identify characteristic features (ridges, lobes, or channels) or excavated blocks related to these rugged flow units. Future 70-cm radar mapping will have an improved signal-to-noise ratio, and thus penetration depth, to reveal greater detail of the buried terrains.

References

Boyce, J. M. (1976), Ages of flows in the lunar nearside maria based on Lunar Orbiter IV photographs, *Proc. Lunar Sci. Conf.*, *VII*, 2717–2746.

Campbell, B. A., B. R. Hawke, and T. W. Thompson (1997), Long-wavelength radar studies of the lunar maria, *J. Geophys. Res.*, *102*, 19,307–19,320, doi:10.1029/97JE00858.

Campbell, B. A., et al. (2007), Focused 70-cm radar mapping of the Moon, *IEEE Trans. Geosci. Remote Sens.*, *45*, 4032–4042, doi:10.1109/TGRS.2007.906582.

Campbell, B. A., B. R. Hawke, and D. B. Campbell (2009), Surface morphology of domes in the Marius Hills and Mons Rumker regions of the Moon from Earth-based radar data, *J. Geophys. Res.*, *114*, E01001, doi:10.1029/2008JE003253.

Carrier, W. D., III, G. R. Olhoeft, and W. Mendell (1991), Physical properties of the lunar surface, in *Lunar Sourcebook: A User's Guide to the Moon*, edited by G. H. Heiken, D. T. Vaniman, and H. H. Schmitt, chap. 9, pp. 475–594, Cambridge Univ. Press, Cambridge, U. K.

Carter, L. M., B. A. Campbell, B. R. Hawke, D. B. Campbell, and M. C. Nolan (2009), Radar remote sensing of pyroclastic deposits in the southern Mare Serenitatis and Mare Vaporum regions of the Moon, *J. Geophys. Res.*, *114*, E11004, doi:10.1029/2009JE003406.

Casella, C. J., and A. B. Binder (1972), Geologic map of the Cleomedes quadrangle of the Moon, *U.S. Geol. Surv.* Map, I-707.

Gifford, A. W., and F. El-Baz (1981), Thickness of lunar mare flow fronts, *Earth Moon Planets*, *24*, 391–398, doi:10.1007/BF00896904.

Gillis, J. J., B. L. Joliff, and R. C. Elphic (2003), A revised algorithm for calculating TiO2 from Clementine UVVIS data: A synthesis of rock, soil, and remotely sensed TiO_2 concentrations, *J. Geophys. Res.*, *108*(E2), 5009, doi:10.1029/2001JE001515.

Hackwill, T. J., J. Guest, and P. D. Spudis (2006), Stratigraphy and evolution of basalts in Mare Humorum and southeastern Procellarum, *Meteorit. Planet. Sci.*, *41*, 479–488.

Harmon, J. K., R. E. Arvidson, E. A. Guinness, B. A. Campbell, and M. A. Slade (1999), Mars mapping with delay-Doppler radar, *J. Geophys. Res.*, *104*, 14,065–14,090, doi:10.1029/1998JE900042.

Hiesinger, H. R., R. Jaumann, G. Neukum, and J. W. Head (2000), Ages of mare basalts on the lunar nearside, *J. Geophys. Res.*, *105*, 29,239–29,275, doi:10.1029/2000JE001244.

Hiesinger, H. R., J. W. Head, U. Wolf, R. Jaumann, and G. Neukum (2003), Ages and stratigraphy of mare basalts in Oceanus Procellarum, Mare Nubium, Mare Cognitum, and Mare Insularum, *J. Geophys. Res.*, *108*(E7), 5065, doi:10.1029/2002JE001985.

Keszthelyi, L., T. Thordarson, A. McEwen, H. Haack, M. Guilbaud, S. Self, and M. J. Rossi (2004), Icelandic analogs to Martian flood lavas, *Geochem. Geophys. Geosyst.*, *5*, Q11014, doi:10.1029/2004GC000758.

Lucey, P. G., D. T. Blewett, and B. D. Joliff (2000), Lunar iron and titanium abundance algorithms based on final processing of Clementine ultraviolet-visible images, *J. Geophys. Res.*, *105*, 20,297–20,306, doi:10.1029/1999JE001117.

McKay, D. S., G. Heiken, A. Basu, G. Blanford, S. Simon, R. Reedy, B. M. French, and J. Papike (1991), The lunar regolith, in *Lunar Sourcebook: A User's Guide to the Moon*, edited by G. H. Heiken, D. T. Vaniman, and H. H. Schmitt, chap. 7, pp. 285–356, Cambridge Univ. Press, Cambridge, U. K.

Rutherford, M. J., P. C. Hess, and G. H. Daniel (1974), Experimental liquid line of descent and liquid immiscibility for basalt 70017, *Proc. Lunar Sci. Conf.*, *V*, 569–583.

Schaber, G. G., T. W. Thompson, and S. H. Zisk (1975), Lava flows in Mare Imbrium: An evaluation of anomalously low Earth-based radar reflectivity, *Moon*, *13*, 395–423, doi:10.1007/BF02626384.

Schaber, G. G., J. M. Boyce, and H. J. Moore (1976), The scarcity of mappable flow lobes on the lunar surface: Unique morphology of the Imbrium flows, *Proc. Lunar Planet. Sci. Conf.*, *VII*, 767–769.

Schaber, G. G., C. Elachi, and T. G. Farr (1980), Remote sensing of SP Mountain and SP lava flow in north-central Arizona, *Remote Sens. Environ.*, *9*, 149–170, doi:10.1016/0034-4257(80)90005-X.

Shorthill, R. W. (1973), Infrared atlas charts of the eclipsed Moon, *Earth Moon Planets*, *7*, 22–45.

Thompson, T. W., R. W. Shorthill, E. A. Whitaker, and S. H. Zisk (1974), Mare Serenitatis: A preliminary definition of surface units by remote observations, *Moon*, *9*, 89–96, doi:10.1007/BF00565395.

Weill, D. F., R. A. Grieve, I. S. McCallum, and Y. Bottinga (1971), Mineralogy-petrology of lunar samples: Microprobe studies of samples 1 2021 and 12022; viscosity of melts of selected lunar compositions, *Proc. Lunar Sci. Conf. II*, 413–430.

Whitaker, E. A. (1972), Lunar color boundaries and their relationship to topographic features: A preliminary survey, *Moon*, *4*, 348–355, doi:10.1007/BF00562002.

_____

B. A. Campbell and L. M. Carter, Center for Earth and Planetary Studies, Smithsonian Institution, MRC 315, PO Box 37012, Washington, DC 20013–7012, USA. (campbellb@si.edu)

D. B. Campbell, NAIC, Cornell University, Ithaca, NY 14853, USA.

R. R. Ghent, Department of Geology, University of Toronto, Toronto, ON M5S 3B1, Canada.

B. R. Hawke, HIGP, University of Hawai'i at Mānoa, Honolulu, HI 96822, USA.